Available online at www.sciencedirect.com
ScienceDirect
Physica C 456 (2007) 160–169
PHYSICA C
www.elsevier.com/locate/physc

Review

Limits of the upper critical field in dirty two-gap superconductors

A. Gurevich

National High Magnetic Field Laboratory, Florida State University, Tallahassee, FL 32310, USA

Received 3 December 2006; accepted 11 January 2007
Available online 25 January 2007

Abstract

An overview of the theory of the upper critical field in dirty two-gap superconductors, with a particular emphasis on MgB_2 is given. We focus here on the maximum H_{c2} which may be achieved by increasing intraband scattering, and on the limitations imposed by weak interband scattering and paramagnetic effects. In particular, we discuss recent experiments which have demonstrated tenfold increase of H_{c2} in dirty carbon-doped films as compared to single crystals, so that $H_{c2}(0)$ parallel to the *ab* planes may approach the BCS paramagnetic limit, $H_p\,[\mathrm{T}] = 1.84T_c\,[\mathrm{K}] \simeq 60$–$70$ T. New effects produced by weak interband scattering in the two-gap Ginzburg–Landau equations and features of $H_{c2}(T)$ in ultrathin MgB_2 films are addressed.

PACS: 74.20.De; 74.20.Hi; 74.60.−w

Keywords: MgB_2; Two-gap superconductivity; Upper critical field; Paramagnetic limit; Impurity scattering

Contents

1. Introduction

It is now well established that superconductivity in MgB_2 with the unexpectedly high critical temperature $T_c \approx 40$ K [1], is due to strong electron–phonon interaction with in-plane boron vibration modes. Extensive ab initio calculations [2–4], along with many experimental evidences from STM, point contact, and Raman spectroscopy, heat capacity, magnetization and rf measurements [5,6] unambiguously indicate that MgB_2 exhibits a two-gap s-wave superconductivity [7,8]. MgB_2 has two distinct superconducting gaps: the main gap $\Delta_\sigma(0) \approx 7.2$ mV, which resides on the 2D cylindrical parts of the Fermi surface formed by in-plane σ antibonding p_{xy} orbitals of B, and the smaller gap $\Delta_\pi(0) \approx 2.3$ mV on the 3D tubular part of the Fermi

E-mail address: gurevich@asc.magnet.fsu.edu

0921-4534/$ - see front matter © 2007 Elsevier B.V. All rights reserved.
doi:10.1016/j.physc.2007.01.008

surface formed by out-of-plane π bonding and antibonding p_z orbitals of B.

The discovery of MgB_2 has renewed interest in new effects of two-gap superconductivity, motivating different groups to take closer looks at other known materials, such as YNi_2B_2C and $LuNi_2B_2C$ borocarbides [9], Nb_3Sn [10], or $NbSe_2$ [11], heavy-fermion [12] and organic [13] superconductors, for which evidences of the two-gap behavior have been reported. However, several features of MgB_2 set it apart from other two-gap superconductors. Not only does MgB_2 have the highest T_c among all non-cuprate superconductors, it also has two coexisting order parameters $\Psi_\sigma = \Delta_\sigma \exp(i\theta_1)$ and $\Psi_\pi = \Delta_\pi \exp(i\theta_2)$, which are *weakly coupled*. The latter is due to the fact that the σ and π bands are formed by two orthogonal sets of in-plane and out-of-plane atomic orbitals of boron, so all overlap integrals, which determine matrix elements of interband coupling and interband impurity scattering are strongly reduced [14]. This feature can result in new effects, which are very important both for the physics and applications of MgB_2. Indeed, two weakly coupled gaps result in an *intrinsic Josephson effect*, which can manifest itself in low-energy interband Josephson plasmons (the Legget mode) [15] with frequencies smaller than $\Delta_\pi/\hbar$. Moreover, strong static electric fields and currents can decouple the bands due to formation of interband textures of 2π planar phase slips in the phase difference $\theta(x) = \theta_1 - \theta_2$ [16,17] well below the global depairing current. In turn, the weakness of interband impurity scattering makes it possible to radically increase the upper critical field H_{c2} by selective alloying of Mg and B sites with nonmagnetic impurities.

Despite the comparatively high T_c, the upper critical field of MgB_2 single crystals is rather low and anisotropic with $H_{c2}^{\perp}(0) \simeq 3$–5 T and $H_{c2}^{\parallel}(0) \simeq 15$–19 T of [5,6], where the indices ⊥ and ∥ correspond to the magnetic field **H** perpendicular and parallel to the *ab* plane, respectively. Since these H_{c2} values were significantly lower than $H_{c2}(0) \simeq 30$ T for Nb_3Sn [18,19], there had been initial scepticism about using MgB_2 as a high-field superconductor, until several groups undertook the well-established procedure of H_{c2} enhancement by alloying MgB_2 with nonmagnetic impurities. The high-field measurements on dirty MgB_2 films and bulk samples have shown up to tenfold increase of $H_{c2}^{\perp}$ as compared to single crystals [20–31], particularly in carbon-doped thin films [28] made by hybrid physico-chemical vapor deposition [32]. This unexpectedly strong enhancement of $H_{c2}(T)$ results from its anomalous upward curvature, rather different from that of $H_{c2}(T)$ for one-gap dirty superconductors [33–36]. As shown in Fig. 1, H_{c2} of MgB_2 C-doped films has already surpassed H_{c2} of Nb_3Sn, which could make cheap and ductile MgB_2 an attractive material for high field applications [37].

This radical enhancement of H_{c2} shown in Fig. 1 is indeed assisted by the features of two-gap superconductivity in MgB_2. Fig. 2 gives another example of $H_{c2}(T)$ for a fiber-textured film [25], which exhibits an upward curvature of $H_{c2}(T)$ for $H \| c$. This behavior of $H_{c2}(T)$ and the anomalous temperature-dependent anisotropy ratio $\Gamma(T) = H_{c2}^{\parallel}(T)/H_{c2}^{\perp}(T)$ are different from that of the one-gap theory in which $H_{c2}(T)$ has a downward curvature, while the slope $H'_{c2} = dH_{c2}/dT$ at T_c is proportional to the normal state residual resistivity ρ_n, and $H_{c2}(0) = 0.69 T_c H'_{c2}$ [33–36]. However, the behavior of $H_{c2}(T)$ in MgB_2 can be explained by the two-gap theory in the dirty limit based on either Usadel [38,39] or Eliashberg [9,40] equations.

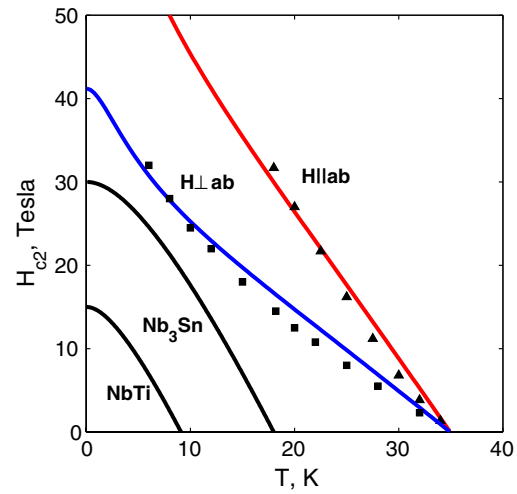

Fig. 1. $H_{c2}(T)$ for carbon-doped MgB_2 films [28] in comparison with NbTi and Nb_3Sn. The red and blue lines show fits from Eq. (19) with $g = 0.045$. (For interpretation of the references in color in this figure legend, the reader is referred to the web version of this article.)

The behavior of $H_{c2}(T)$ can be qualitatively understood using a simple bilayer model shown in Fig. 3, which captures the physics of two-gap superconductivity in MgB_2, and suggests ways by which H_{c2} can be further increased. Indeed, MgB_2 can be mapped onto a bilayer in which two thin films corresponding to σ and π bands are separated by a Josephson contact, which models the interband

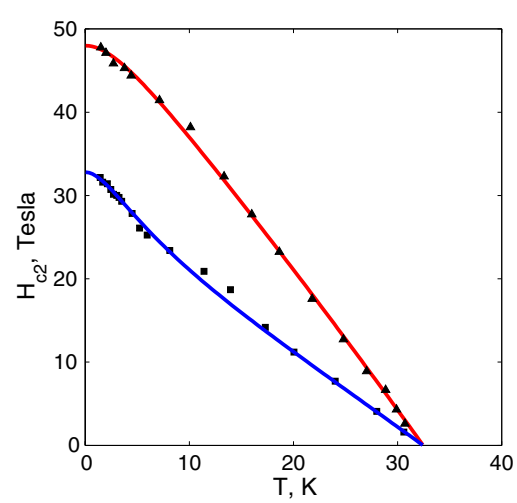

Fig. 2. $H_{c2}(T)$ of a fiber-textured MgB_2 film [25] both parallel (triangles) and perpendicular (squares) to the *ab* planes. The solid lines show calculations from Eq. (19) with $g = 0.065$, $D_\pi \ll D_\sigma^{(ab)}$ for $H \| c$ and $D_\pi = 0.19(D_\sigma^{(c)} D_\sigma^{(ab)})^{1/2}$ for $H \perp c$.

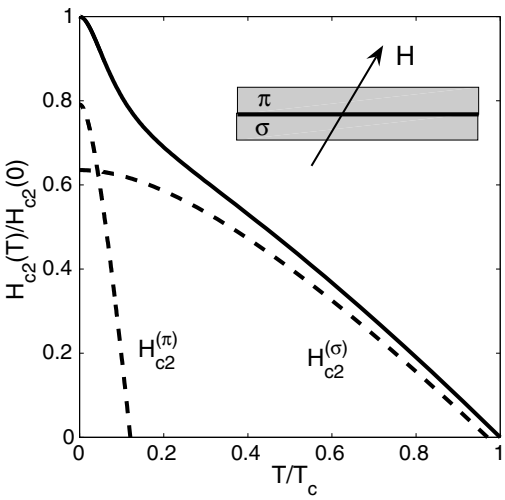

Fig. 3. The mechanism of the upward curvature of $H_{c2}(T)$ illustrated by the bilayer toy model shown in the inset. The dashed curves show $H_{c2}(T)$ calculated for σ and π films in the one-gap dirty limit with the BCS coupling constants $\lambda_\sigma = 0.81$, $\lambda_\pi = 0.285$, and $D_\pi = 0.1D_\sigma$. The solid curve shows $H_{c2}(T)$ calculated from Eq. (25) of the two-gap dirty limit theory for the BCS matrix constants from Ref. [77].

coupling. The global $H_{c2}(T)$ of this weakly-coupled bilayer is mostly determined by the film with the highest H_{c2}, even if $T_c^{(\sigma)}$ and $T_c^{(\pi)}$ are very different. For example, if the π film is much dirtier than the σ film then $H_{c2}^{(\sigma)}$ dominates at higher T, but at lower temperatures the π film takes over, resulting in the upward curvature of $H_{c2}(T)$. If the σ film is dirtier, the π film only results in a slight shift of the H_{c2} curve and a reduction of the slope H'_{c2} near T_c.

The bilayer model also clarifies the anomalous angular dependence of $H_{c2}(\alpha, T)$ for **H** inclined by the angle α with respect to the c-axis (parallel to the film normal in Fig. 3) [41]. In this case both $H_{c2}^{(\sigma)}(\alpha, T)$ and $H_{c2}^{(\pi)}(\alpha, T)$ depend on α according to the temperature-independent one-gap scaling $H_{c2}(\alpha) = H_{c2}(0, T)/\sqrt{\cos^2\alpha + \epsilon\sin^2\alpha}$ [42,43], but with very different effective mass ratios $\epsilon = m_{ab}/m_c$ for each film. Because the σ band is much more anisotropic than the π band, $\epsilon_\sigma \ll 1$, and $\epsilon_\pi \sim 1$ [44,45], the one-gap angular scaling for the global $H_{c2}(\alpha, T)$ breaks down. For example, in the case shown in Fig. 3, $H_{c2}(T)$ is anisotropic at higher T, but at lower T, the nearly isotropic π band reduces the overall anisotropy of H_{c2}, so the ratio $\Gamma(T) = H_{c2}^{\parallel}(T)/H_{c2}^{\perp}(T)$ *decreases* as T decreases. This is characteristic of many dirty MgB_2 films like the one shown in Fig. 2, for which the π band is typically much dirtier than the σ band. By contrast, in clean MgB_2 single crystals $\Gamma(T)$ increases from ≃2–3 near T_c to ≃5–6 at $T \ll T_c$ [46–56]. This behavior was explained by two-gap effects in the clean limit [57,58].

Fig. 3 suggests that $H_{c2}(T)$ of MgB_2 can be significantly increased at low T by making the π band much dirtier than the main σ band. This could be done by disordering the Mg sublattice, thus disrupting the p_z boron out-of-plane orbitals, which form the π band. Achieving high H_{c2} requires that both σ and π bands are in the dirty limit. Yet, making the π band much dirtier than the σ band provides a "free boost" in H_{c2} without too much penalty in T_c suppression due to pairbreaking interband scattering or band depletion due to doping [59,60]. In fact, the interband scattering is weak for the same reason that Ψ_σ and Ψ_π are weakly coupled, which may enable alloying MgB_2 with more impurities to achieve higher H_{c2}. Systematic incorporation of impurities in MgB_2 has not been yet achieved because the complex substitutional chemistry of MgB_2 is still poorly understood [61–64]. Several groups have reported a significant increase of H_{c2} by irradiation with protons [65], neutrons [66,67] or heavy ions [68], but so far the carbon impurities have been the most effective to provide the huge H_{c2} enhancement shown in Figs. 1 and 2. The effect of carbon on different superconducting properties can be rather complex [69–71] and still far from being fully understood. Yet given the indisputable benefits of carbon alloying, one can pose the basic question: how far can H_{c2} be further increased?

The bilayer model suggests that H_{c2} increases if intraband scattering is enhanced. However, because intraband impurity scattering causes an admixture of pairbreaking interband scattering, the first question is to what extent weak interband scattering in MgB_2 can limit H_{c2}. Another important question is how far is the observed H_{c2} from the paramagnetic limit H_p? In the BCS theory H_p is defined by the condition: $\mu_B H_p^{BCS} = \Delta/\sqrt{2}$, or H_p^{BCS} [T] $= 1.84T_c$ [K] [72], where μ_B is the Bohr magneton. For $T_c = 35$ K, this yields $H_p = 65$ T, not that far from the zero-field $H_{c2}^{\parallel}(0)$ in Figs. 1 and 2. However, the BCS model underestimates H_p, which is significantly enhanced by strong electron–phonon coupling [73]:

$$H_p \simeq (1 + \lambda_{ep})H_p^{BCS}, \tag{1}$$

where λ_{ep} is the electron–phonon constant. Taking $\lambda_{ep} \approx 1$ for the σ band [2,3], we obtain $H_p \sim 130$ T, so there still a large room for increasing H_{c2} by optimizing the intra and interband impurity scattering. For instance, increasing H'_{c2} to a rather common for many high field superconductors value of 2 T/K (much lower than $H'_{c2} \simeq$ 5–14 T/K for $PbMo_6S_8$ [74]) could drive H_{c2} of MgB_2 with $T_c \simeq 35$ K above 70 T. In the following we give a brief overview of recent results in the theory of dirty two-gap superconductors focusing on new effects brought by weak interband scattering and paramagnetic effects. The main conclusion is that, although interband scattering in MgB_2 is indeed weak, it cannot be neglected in calculations of $H_{c2}(T)$. We will also address the crossover from the orbitally-limited to the paramagnetically limited H_{c2} in a two-gap superconductor.

2. Two-gap superconductors in the dirty limit

We regard MgB_2 as a dirty anisotropic superconductor with two sheets 1 and 2 of the Fermi surface on which the superconducting gaps take the values Δ_1 and Δ_2, respectively (indices 1 and 2 correspond to σ and π bands).

Although the σ band is anisotropic, MgB_2 is not a layered material [75,76], so the continuum BCS theory is applicable because the c-axis coherence length ξ_c is much longer than the spacing between the boron planes ~3.5 Å. Indeed, even for $H_{c2}^{\perp}(0) = 40$ T and $H_{c2}^{\parallel}(0) = 60$ T in Fig. 1, the anisotropic Ginzburg–Landau (GL) theory [42] gives $\xi_c = (\phi_0 H_{c2}^{\perp}/2\pi)^{1/2}/H_{c2}^{\parallel} \approx 19$ Å. Strong coupling in MgB_2 should be described by the Eliashberg equations [40], but we consider here manifestations of intra and interband scattering and paramagnetic effects in H_{c2} using the more transparent two-gap Usadel equations [38]:

$$\omega f_1 - \frac{D_1^{\alpha\beta}}{2}[g_1 \Pi_\alpha \Pi_\beta f_1 - f_1 \nabla_\alpha \nabla_\beta g_1] = \Psi_1 g_1 + \gamma_{12}(g_1 f_2 - g_2 f_1) \quad (2)$$

$$\omega f_2 - \frac{D_2^{\alpha\beta}}{2}[g_2 \Pi_\alpha \Pi_\beta f_2 - f_2 \nabla_\alpha \nabla_\beta g_2] = \Psi_2 g_2 + \gamma_{21}(g_2 f_1 - g_1 f_2), \quad (3)$$

Here the Usadel Green's functions $f_m(\mathbf{r},\omega)$ and $g_m(\mathbf{r},\omega)$ in the mth band depend on $\mathbf{r}$ and the Matsubara frequency $\omega = \pi T(2n+1)$, $D_m^{\alpha\beta}$ are the intraband diffusivities due to nonmagnetic impurity scattering, $2\gamma_{mm'}$ are the interband scattering rates, $\mathbf{\Pi} = \nabla + 2\pi i\mathbf{A}/\phi_0$, $\mathbf{A}$ is the vector potential, and ϕ_0 is the flux quantum. Eqs. (2) and (3) are supplemented by the equations for the order parameters $\Psi_m = \Delta_m \exp(i\varphi_m)$,

$$\Psi_m = 2\pi T \sum_{\omega>0}^{\omega_D} \sum_m \lambda_{mm'} f_{m'}(\mathbf{r},\omega), \quad (4)$$

normalization condition $|f_m|^2 + g_m^2 = 1$, and the supercurrent density

$$J^\alpha = -2\pi e T \mathrm{Im} \sum_\omega \sum_m N_m D_m^{\alpha\beta} f_m^* \Pi_\beta f_m. \quad (5)$$

Here N_m is the partial electron density of states for both spins in the mth band, and α and β label the Cartesian indices. Eq. (4) contains the matrix of the BCS coupling constants $\lambda_{mm'} = \lambda_{mm'}^{(ep)} - \mu_{mm'}$, where $\lambda_{mm'}^{(ep)}$ are electron–phonon constants, and μ'_{mm} is the Coulomb pseudopotential. The diagonal terms λ_{11} and λ_{22} quantify intraband pairing, and λ_{12} and λ_{21} describe interband coupling. Hereafter, the following *ab initio* values $\lambda_{\sigma\sigma} \approx 0.81$, $\lambda_{\pi\pi} \approx 0.285$, $\lambda_{\sigma\pi} \approx 0.119$, and $\lambda_{\pi\sigma} \approx 0.09$ [77] are used. There are also the symmetry relations:

$$N_1\lambda_{12} = N_2\lambda_{21}, \quad N_1\gamma_{12} = N_2\gamma_{21} \quad (6)$$

where $N_\pi \approx 1.3N_\sigma$ for MgB_2. Solutions of Eqs. (2) and (6) minimize the following free energy $\int F d^3\mathbf{r}$ [17]:

$$F = \frac{1}{2}\sum_{mm'} N_m \Psi_m \Psi_m^* \lambda_{mm'}^{-1} + F_1 + F_2 + F_i \quad (7)$$

Here F_1 and F_2 are intraband contributions,

$$F_m = 2\pi T \sum_{\omega>0} N_m[\omega(1-g_m) - \mathrm{Re}(f_m^* \Delta_m) + D_m^{\alpha\beta}[\Pi_\alpha f_m \Pi_\beta^* f_m^* + \nabla_\alpha g_m \nabla_\beta]g_m/4] \quad (8)$$

and F_i is due to interband scattering [78]:

$$F_i = 2\pi q T \sum_{\omega>0}[1 - g_1 g_2 - \mathrm{Re}(f_1^* f_2)], \quad (9)$$

where $2q = N_1\gamma_{12} + N_2\gamma_{21}$. The Usadel equations result from $\delta F/\delta f_m^* = 0$, $\partial F/\partial \Psi_m^* = 0$, and $\mathbf{J} = -c\delta F/\delta \mathbf{A}$. Taking $f_m = \sin\alpha_m$ and $g_m = \cos\alpha_m$, we obtain

$$\omega \sin\alpha_1 + \gamma_{12}\sin(\alpha_1 - \alpha_2) = \Delta_1 \cos\alpha_1, \quad (10)$$

$$\omega \sin\alpha_2 + \gamma_{21}\sin(\alpha_2 - \alpha_1) = \Delta_2 \cos\alpha_2. \quad (11)$$

These coupled equations along with Eq. (4) define the two-gap uniform states for $J = 0$.

3. Critical temperature

Eqs. (2) and (3) give the well-known results for T_c in two-gap superconductors [7,8,79,80]. For negligible interband scattering, the substitution of $f_1 = \Delta_1/\omega$ and $f_2 = \Delta_2/\omega$ into Eq. (4) yields:

$$T_{c0} = 1.14\hbar\omega_D \exp[-(\lambda_+ - \lambda_0)/2w], \quad (12)$$

where $\lambda_\pm = \lambda_{11} \pm \lambda_{22}$, $w = \lambda_{11}\lambda_{22} - \lambda_{12}\lambda_{21}$, and $\lambda_0 = (\lambda_-^2 + 4\lambda_{12}\lambda_{21})^{1/2}$. The interband coupling increases T_{c0} as compared to noninteracting bands ($\lambda_{12} = \lambda_{21} = 0$), while intraband impurity scattering does not affect T_{c0}, in accordance with the Anderson theorem. Solving the linearized Eqs. (2) and (3) with $\gamma'_{mm} \neq 0$, gives T_c with the account of pairbreaking interband scattering:

$$U\left(\frac{g}{t_c}\right) = -\frac{(\lambda_0 + w\ln t_c)\ln t_c}{p + w\ln t_c}, \quad (13)$$

$$2p = \lambda_0 + [\gamma_-\lambda_- - 2\lambda_{21}\gamma_{12} - 2\lambda_{12}\gamma_{21}]/\gamma_+, \quad (14)$$

$$U(x) = \psi(1/2 + x) - \psi(1/2), \quad (15)$$

where $t_c = T_c/T_{c0}$ and $\gamma_\pm = \gamma_{12} \pm \gamma_{21}$, $g = \gamma_+/2\pi T_{c0}$, and $\psi(x)$ is a digamma function. The dependence of T_c on the interband scattering parameter g is shown in Fig. 4. As $g \to \infty$, Eqs. (13) and (14) give $T_c \to T_{c0}\exp(-p/w)$, and for $g \ll 1$, we have

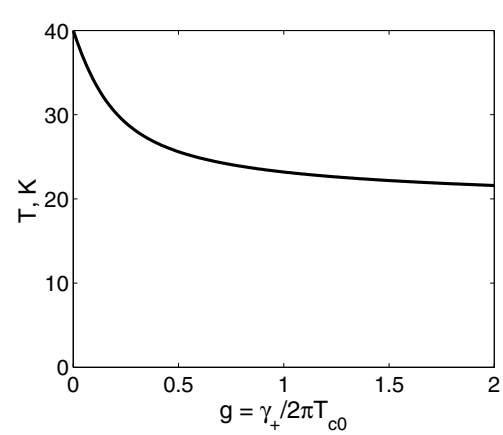

Fig. 4. Dependence of the critical temperature T_c on the interband scattering parameter g calculated from Eq. (13) with the BCS matrix constants λ_{mn} from Ref. [77].

$$T_c = T_{c0} - \frac{\pi}{8\lambda_0}[\lambda_0\gamma_+ + \lambda_-\gamma_- - 2\lambda_{21}\gamma_{12} - 2\lambda_{12}\gamma_{21}] \quad (16)$$

This formula can be used to extract the interband scattering rates from a small shift of T_c [81]. However, as shown below, even weak interband scattering can significantly change the behavior of $H_{c2}(T)$, so it cannot be neglected even though $g \ll 1$.

4. Upper critical field for H||c

H_{c2} along the c-axis is the maximum eigenvalue of the linearized Eqs. (2) and (3):

$$(\omega \pm i\mu_B H)f_1 - \frac{D_1}{2}\Pi^2 f_1 = \Delta_1 + (f_2 - f_1)\gamma_{12}, \quad (17)$$

$$(\omega \pm i\mu_B H)f_2 - \frac{D_2}{2}\Pi^2 f_2 = \Delta_2 + (f_1 - f_2)\gamma_{21}. \quad (18)$$

Here the Zeeman paramagnetic term $\pm\mu_B H$, which requires summation over both spin orientations in Eq. (4), is included. In the gauge $A_y = Hx$, the solutions are $f_m(x) = \tilde{f}_m \exp(-\pi H x^2/\phi_0)$, and $\Delta_m(x) = \tilde{\Delta}_m \exp(-\pi H x^2/\phi_0)$, where $\tilde{f}_m$ is expressed via $\tilde{\Delta}_m$ from Eqs. (17) and (18). The solvability condition (4) of two linear equations for $\tilde{\Delta}_1$ and $\tilde{\Delta}_2$ gives the equation for H_{c2} [38], which accounts for interband and intraband scattering and paramagnetic effects:

$$(\lambda_0 + \lambda_i)(\ln t + U_+) + (\lambda_0 - \lambda_i)(\ln t + U_-) + 2w(\ln t + U_+)(\ln t + U_-) = 0, \quad (19)$$

where $t = T/T_{c0}$, and

$$\lambda_i = [(\omega_- + \gamma_-)\lambda_- - 2\lambda_{12}\gamma_{21} - 2\lambda_{21}\gamma_{12}]/\Omega_0, \quad (20)$$

$$2\Omega_\pm = \omega_+ + \gamma_+ \pm \Omega_0, \quad (21)$$

$$\Omega_0 = [(\omega_- + \gamma_-)^2 + 4\gamma_{12}\gamma_{21}]^{1/2}, \quad (22)$$

$$\omega_\pm = (D_1 \pm D_2)\pi H/\phi_0, \quad (23)$$

$$U_\pm = \mathrm{Re}\,\psi\left(\frac{1}{2} + \frac{\Omega_\pm + i\mu_B H}{2\pi T}\right) - \psi\left(\frac{1}{2}\right). \quad (24)$$

If interband scattering and paramagnetic effects are negligible, Eqs. (19)–(24) reduce to a simpler equation [38,39], which can be presented in the parametric form:

$$\ln t = -[U(h) + U(\eta h) + \lambda_0/w]/2 + [(U(h) - U(\eta h) - \lambda_-/w)^2/4 + \lambda_{12}\lambda_{21}/w^2]^{1/2}, \quad (25)$$

$$H_{c2} = 2\phi_0 T_c t h/D_1, \quad (26)$$

where $\eta = D_2/D_1$, and the parameter h runs from 0 to ∞ as T varies from T_c to 0. For equal diffusivities, $\eta = 1$, Eq. (25) simplifies to the one-gap de-Gennes–Maki equation $\ln(t) + U(h) = 0$ [34–36].

Now we consider some limiting cases, which illustrate how H_{c2} depends on different parameters. Fig. 5 shows the evolution of H_{c2} as g increases for fixed D_1 and D_2 and negligible paramagnetic effects. Interband scattering reduces the upward curvature of $H_{c2}(T)$, $H_{c2}(0)$, and T_c,

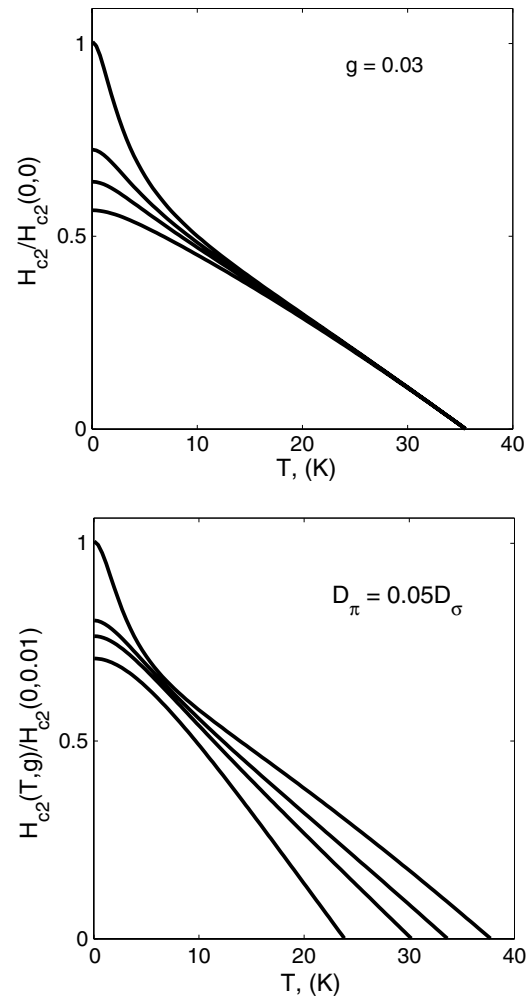

Fig. 5. Effect of interband scattering and the diffusivity ratio on the evolution of $H_{c2}(T)$. Upper panel shows $H_{c2}(T,\eta)$ for the fixed $g = 0.03$ and different $\eta = D_2/D_1$: 0, 0.05, 0.1, 0.5 (from top to bottom curves). Lower panel shows $H_{c2}(T,g)$ for the fixed $D_2/D_1 = 0.05$ and different $g = 0.01, 0.05, 0.1, 0.5$ (from top to bottom curves).

while increasing the slope H'_{c2} at T_c. Notice that the significant changes in the shape of $H_{c2}(T)$ in Fig. 5 occur for weak interband scattering ($g \ll 1$), which also provides a finite $H_{c2}(0)$ even if $D_2 \to 0$. For example, the high-field films in Figs. 1 and 2 have $g \simeq 0.045$ and 0.065, respectively. For $g \ll 1$, Eq. (19) yields the GL linear temperature dependence near T_c:

$$H_{c2} = \frac{8\phi_0(T_c - T)}{\pi^2(s_1 D_1 + s_2 D_2)} \quad (27)$$

where T_c is given by Eq. (16), $s_1 = 1 + \lambda_-/\lambda_0$ and $s_2 = 1 - \lambda_-/\lambda_0$. Eq. (27) is written in the linear accuracy in $g \ll 1$. Higher order terms in g not only shift T_c but also increase the slope H'_{c2} at T_c, as evident from Fig. 5. For $s_1 \sim s_2$, the slope H'_{c2} is mostly determined by the cleanest band with the maximum diffusivity. However, because of weak interband coupling in MgB_2, the values of s_1 and s_2 are very different. For $\lambda_{11} = 0.81$, $\lambda_{22} = 0.285$, $\lambda_{12} = 0.119$, $\lambda_{21} = 0.09$ [77], we get $\lambda_- = \lambda_{11} - \lambda_{22} = 0.525$,

$\lambda_0 = (\lambda_-^2 + 4\lambda_{12}\lambda_{21})^{1/2} = 0.564$, hence $s_1 = 1 + \lambda_-/\lambda_0 = 1.93$, $s_2 = 1 - \lambda_-/\lambda_0 = 0.07$. Thus, H'_{c2} is mostly determined by D_1 of the σ band. Yet, if the σ band is so dirty that $D_1/D_2 < s_2/s_1 \simeq 0.04$, the slope H'_{c2} is determined by the much cleaner π band.

At low T both the Zeeman and interband scattering terms in Eq. (19) can be essential. Eq. (19) reduces to the following equation for $H_{c2}(0)$:

$$(\lambda_0 + \lambda_i)\ln\frac{\mu_B^2 H_p^2}{\mu_B^2 H^2 + \Omega_+^2} + (\lambda_0 - \lambda_i)\ln\frac{\mu_B^2 H_p^2}{\mu_B^2 H^2 + \Omega_-^2} = w\ln\frac{\mu_B^2 H_p^2}{\mu_B^2 H^2 + \Omega_+^2}\ln\frac{\mu_B^2 H_p^2}{\mu_B^2 H^2 + \Omega_-^2} \quad (28)$$

where $\mu_B H_p = \pi T_{c0}/2\gamma$ is the field of paramagnetic instability of the superconducting state, and $\ln\gamma = 0.577$. We first consider the limit $g \to 0$, which defines the maximum $H_{c2}(0)$ achievable in a dirty two-gap superconductor with no T_c suppression. In this case $\Omega_+ = \pi D_1 H/\phi_0$ and $\Omega_- = \pi D_2 H/\phi_0$, so for $T \ll T_c$, paramagnetic effects just renormalize the intraband diffusivities in Eq. (28):

$$D_m \to \widetilde{D}_m = \sqrt{D_m^2 + D_0^2}, \quad (29)$$

where $D_0 = \mu_B\phi_0/\pi$ is the quantum diffusivity

$$D_0 = \hbar/2m, \quad (30)$$

and m is the bare electron mass. Eq. (30) follows from the basic diffusion relation $l^2 = D_0 t$, and the energy uncertainty principle $\hbar^2/2ml^2 = \hbar/t$ for a particle confined in a region of length l. For $g = 0$, Eq. (28) yields

$$H_{c2}(0) = \frac{\phi_0 T_c}{2\gamma\sqrt{\widetilde{D}_1\widetilde{D}_2}}\exp\left(\frac{f}{2}\right), \quad (31)$$

$$f = \left(\frac{\lambda_0^2}{w^2} + \ln^2\frac{\widetilde{D}_2}{\widetilde{D}_1} + \frac{2\lambda_-}{w}\ln\frac{\widetilde{D}_2}{\widetilde{D}_1}\right)^{1/2} - \frac{\lambda_0}{w}. \quad (32)$$

If $D_0 \ll D_m$, Eqs. (31) and (32) reduce to the result of Ref. [38], and for the symmetric case, $\widetilde{D}_1 = \widetilde{D}_2$, Eqs. (31) and (32) give the one-band result $H_{c2}(0) = \phi_0 T_c/2\gamma\widetilde{D}$ [35]. However for $\widetilde{D}_1 \neq \widetilde{D}_2$, $H_{c2}(0)$ can be much higher than $H_{c2}(0) = 0.69 H'_{c2} T_c$. Indeed, if the effective diffusivities, $\widetilde{D}_1$ and $\widetilde{D}_2$ are very different, Eqs. (31) and (32) yield

$$H_{c2}(0) = \frac{\phi_0 T_c}{2\gamma\widetilde{D}_2}e^{-(\lambda_- + \lambda_0)/2w}, \quad \widetilde{D}_2 \ll \widetilde{D}_1 e^{-\frac{\lambda_0}{w}}, \quad (33)$$

$$H_{c2}(0) = \frac{\phi_0 T_c}{2\gamma\widetilde{D}_1}e^{-(\lambda_0 - \lambda_-)/2w}, \quad \widetilde{D}_1 \ll \widetilde{D}_2 e^{-\frac{\lambda_0}{w}}. \quad (34)$$

Thus, $H_{c2}(0)$ is determined by the *minimum* effective diffusivity, but unlike the limit of $D_0 \to 0$, $H_{c2}(0)$ remains finite even for $D_1 \to 0$ or $D_2 \to 0$. In fact, if both $D_1 \ll D_0$ and $D_2 \ll D_0$, we return to the symmetric case $\widetilde{D}_1 = \widetilde{D}_2$, for which Eqs. (31) and (32) yield the result of the one-gap dirty limit theory [36]

$$H_{c2}(0) \to H_p = \phi_0 T_c/2\gamma D_0 = \pi T_c/2\gamma\mu_B \quad (35)$$

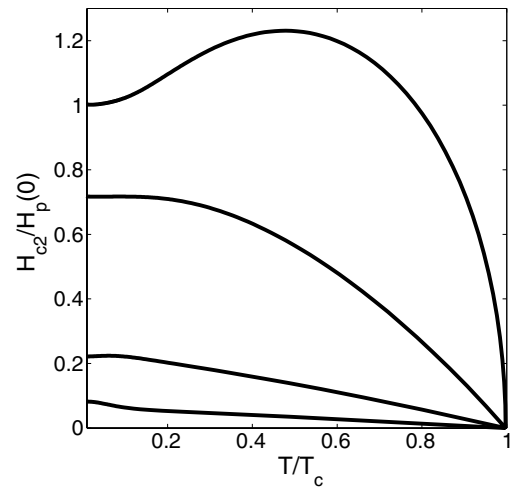

Fig. 6. Crossover from the orbitally to paramagnetically limited $H_{c2}(T)$ calculated from Eqs. (25) and (36), (38) for $D_2 = 0.05D_1$ and $D_1/D_0 = 0, 1, 5, 20$ from top to bottom curves, respectively.

For a one-band superconductor, Eq. (35) can also be written as the paramagnetic pairbreaking condition, $\mu_B H_p = \Delta(0)/2$, where $\Delta(0) = \pi T_c/\gamma$ is the zero-temperature gap. For two-band superconductors, the meaning of H_p is less transparent, yet the maximum H_p expressed via T_c is given by the same Eq. (35) as for one-band superconductors.

Finally we consider how paramagnetic effects affect the shape of $H_{c2}(T)$ in the limit $g \to 0$. This case is described by Eq. (26) modified as follows:

$$U(h) \to \mathrm{Re}\,\psi[1/2 + h(i + p)] - \psi(1/2) \quad (36)$$

$$U(\eta h) \to \mathrm{Re}\,\psi[1/2 + h(p\eta + i)] - \psi(1/2) \quad (37)$$

$$H_{c2} = H_{c2} = 2\phi_0 T_c \mathrm{th}/D_0, \quad (38)$$

where $p = D_1/D_0$, and $\eta = D_2/D_1$. Fig. 6 shows how $H_{c2}(T)$ evolves from the orbitally-limited $H_{c2}(T)$ with an upward curvature at $D_1 \gg D_2$ to the paramagnetically-limited $H_{c2}(T)$ of a one-gap superconductor for $D_1 < D_0$ [72]. The nonmonotonic dependence of $H_{c2}(T)$ in Fig. 6 indicates the first-order phase transition, similar to that in one-gap superconductors.

5. Thin films in a parallel field

H_{c2} can be significantly enhanced in thin films or multilayers, in which MgB_2 layers are separated by nonsuperconducting layers. It is well known that in a thin film of thickness $d < \xi$ in a parallel field, $H_{c2}^{(f)} = 2\sqrt{3}H_{c2}\xi/d$ can be higher than the bulk $H_{c2} = \phi_0/2\pi\xi^2$ [76,82]. Let us see how this result is generalized to two-gap superconductors. For a thin film of thickness $d < \max(\xi_1, \xi_2)$, the functions f_1 and f_2 are nearly constant, so integrating Eqs. (17) and (18) over x with $\partial_x f(\pm d/2) = 0$, results in two linear equations for f_1 and f_2 with $\Pi^2 = (\pi H d/\phi_0)^2/3$. Thus, we obtain the previous Eqs. (19)–(21), (23), (24) in which one should make the replacement

$$\omega_{\pm}^{(f)} \to (\pi H d/\phi_0)^2 (D_1 \pm D_2)/6 \tag{39}$$

We first consider the case of negligible interband scattering and paramagnetic effects. Then Eqs. (19) and (39) give the square-root temperature dependence near T_c

$$H_{c2}^{(f)} = \frac{4\phi_0\sqrt{3T_c(T_c - T)}}{\pi^{3/2} d (s_1 D_1 + s_2 D_2)^{1/2}} \tag{40}$$

characteristic of thin films [82] instead of the bulk GL linear dependence (27). From Eqs. (31) and (39) we can also obtain $H_{c2}^{(f)}(0)$ for $D_0 \ll D_m$:

$$H_{c2}^{(f)}(0) = \frac{\phi_0}{d}\left(\frac{3T_c}{\pi\gamma}\right)^{1/2} \frac{\exp(f/4)}{(D_1 D_2)^{1/4}} \tag{41}$$

Next we consider the crossover to the paramagnetic limit in thin films at low temperatures. For negligible interband scattering, the expressions $\mu_B^2 H^2 + \Omega^2$ under the logarithms in Eq. (28) become $\mu_B^2 H^2 + (\pi H d/\phi_0)^4 D^2/36$. Substituting here $H_{c2}^{(f)} \sim \phi_0/\xi d$, we conclude that paramagnetic effects become essential if

$$\min(D_1, D_2) < D_0 \xi/d. \tag{42}$$

Thus, reducing the film thickness extends the region of the parameters where H_{c2} is limited by the paramagnetic effects rather than by impurity scattering.

6. Anisotropy of H_{c1} and H_{c2}

For anisotropic one-gap superconductors, the angular dependence of the lower and the upper critical fields is given by [42,43]

$$H_{c1}(\alpha, T) = \frac{H_{c1}(0,T)}{R(\alpha)}, \quad H_{c2}(\alpha, T) = \frac{H_{c2}(0,T)}{R(\alpha)} \tag{43}$$

where $R(\alpha) = (\cos^2\alpha + \epsilon\ \sin^2\alpha)^{1/2}$, $\epsilon = m_{ab}/m_c$. Here the anisotropy parameter $\Gamma(T) = H_{c2}^{\parallel}/H_{c2}^{\perp} = \epsilon^{-1/2}$ is independent of T for both H_{c1} and H_{c2}. By contrast, $\Gamma_2(T) = H_{c2}^{\parallel}/H_{c2}^{\perp}$ for MgB_2 single crystals increases from ~2–3 at T_c to 5–6 at $T \ll T_c$, but $\Gamma_1(T) = H_{c1}^{\parallel}/H_{c1}^{\perp}$ decreases from ≃2–3 to ≃1 as T decreases [46–56]. This behavior was explained by the two-gap theory in the clean limit [57,58,83,84].

The dirty limit is more intricate in the sense that $\Gamma(T)$ can either increase or decrease with T, depending on the diffusivity ratio D_2/D_1. However, the physics of this dependence is rather transparent and can be understood using the bilayer toy model as discussed in the Introduction. Indeed, for very different D_1 and D_2, both the angular and the temperature dependencies of $H_{c2}(\alpha, T)$ are controlled by cleaner band at high T and by dirtier band at lower T. For instance, if $D_2 \ll D_1$, the high-T part of $H_{c2}(\alpha, T)$ is determined by the anisotropic σ band, while the low-T part is determined by the isotropic π band. In this case $\Gamma_2(T)$ decreases as T decreases, as characteristic of dirty MgB_2 films represented in Figs. 1 and 2. If the π band is cleaner than the σ band, $\Gamma_2(T)$ increases as T decreases, similar to single crystals.

For the field **H** inclined with respect to the c-axis, the first Landau level eigenfunction no longer satisfies Eqs. (17), (18) and (4). In this case $f_m(\omega, \mathbf{r})$ are to be expanded in full sets of eigenfunctions for all Landau levels, and H_{c2} becomes a root of a matrix equation $\hat{M}(H_{c2}) = 0$ [38,39]. As shown in Ref. [38], this matrix equation for H_{c2} greatly simplifies for the moderate anisotropy characteristic of dirty MgB_2 for which all formulas of the previous section can also be used for the inclined field as well by replacing D_1 and D_2 with the angular-dependent diffusivities $D_1(\alpha)$ and $D_2(\alpha)$ for *both bands*:

$$D_m(\alpha) = [D_m^{(a)2}\cos^2\alpha + D_m^{(a)} D_m^{(c)} \sin^2\alpha]^{1/2} \tag{44}$$

In terms of the bilayer model shown in Fig. 1, Eq. (44) just means that Eq. (43) should be applied separately for each of the films. For $g = 0$, Eqs. (27) and (44) determine the angular dependence of $H_{c2}(\alpha)$ near T_c, and the London penetration depth $\Lambda_{\alpha\beta}$ is given by [38]

$$\Lambda_{\alpha\beta}^{-2} = \frac{4\pi^4}{\phi_0^2}\left[N_1 D_1^{\alpha\beta}\Delta_1 \tanh\frac{\Delta_1}{2T} + N_2 D_2^{\alpha\beta}\Delta_2 \tanh\frac{\Delta_2}{2T}\right] \tag{45}$$

Eqs. (27), (44) and (60) show that the one-gap scaling (43) breaks down because the behavior of $H_{c1}(\alpha, T)$ is mostly controlled by the cleaner band for all T, while the behavior of $H_{c2}(\alpha, T)$ is determined by the cleaner band at higher T, and by the dirtier band at lower T. Thus, $\Gamma_1(T)$ and $\Gamma_2(T)$ for H_{c1} and H_{c2} in the two-gap dirty limit are different. Temperature dependencies of $\Gamma(T)$ were calculated in Refs. [38,39].

Eqs. (44) and (19) describe well both the temperature and the angular dependencies of $H_{c2}(\alpha, T)$ in dirty MgB_2 films [25,28–30]. Eq. (44) is valid if the σ band is not too anisotropic, and the off-diagonal elements $M_{mn} \sim \zeta^{m+n}$ are negligible provided that $\zeta \ll 1$ [38]. Here

$$\zeta = \frac{(\epsilon_1 - \epsilon_2)^2 \sin^4\alpha}{[\sqrt{\cos^2\alpha + \epsilon_1 \sin^2\alpha} + \sqrt{\cos^2\alpha + \epsilon_2 \sin^2\alpha}]^4}, \tag{46}$$

$\epsilon_1 = D_1^{(c)}/D_1^{(ab)}$ and $\epsilon_2 = D_2^{(c)}/D_2^{(ab)}$. For $\epsilon_2 = 1$, the parameter $\zeta(\alpha) < 0.45$ for a rather strong anisotropy $\epsilon_1 < 0.04$ and $\alpha = \pi/2$. For a stronger anisotropy, the condition $\zeta(\alpha) \ll 1$ can still hold in a wide range of α, except a vicinity of $\alpha \approx \pi/2$. In this case the calculation of $H_{c2}(\alpha, T)$ requires a numerical solution of the matrix equation for H_{c2} [39]. However, the Usadel theory can only be applied to dirty MgB_2 samples which, contrary to the assumption of Ref. [39], usually exhibit much weaker anisotropy ($\Gamma_2 \simeq 1$–2) than single crystals. Perhaps, strong impurity scattering and admixture of interband scattering reduce the anisotropy of $D_1^{(c)}/D_1^{(ab)} \simeq 0.2$–0.3 as compared to that of the Fermi velocities $\langle v_c^2\rangle_\sigma/\langle v_{ab}^2\rangle_\sigma \sim 0.02$ predicted by *ab initio* calculations for single crystals [44]. The moderate anisotropy of D_1 in dirty MgB_2 makes the scaling rule (44) a very good approximation, as was recently confirmed experimentally [30].

7. Ginzburg–Landau equations

The two-gap GL equations were obtained both for the dirty limit without interband scattering [38,85], and for the clean limit [86]. Here we consider the GL dirty limit, focusing on new effects brought by interband scattering. For $\gamma_{mm'} = 0$, the Usadel equations near T_c yield

$$f_m = \Psi_m/\omega + D_{m\alpha}\Pi_\alpha^2\Psi/2\omega^2 - \Psi_m|\Psi_m|^2/2\omega^3, \tag{47}$$

where the principal axis of $D_{\alpha\beta}$ are taken along the crystalline axis. For weak interband scattering, the free energy $F = F_0 + F_i$ contains the free energy $F_0\{\Psi_1, \Psi_2\}$ for $\gamma_{mm'} = 0$ and the correction $F_i\{\Psi_1, \Psi_2\}$ linear in $\gamma_{mm'}$. Here F_0 does not have first-order corrections in $\gamma_{mm'}$ if Ψ_m satisfies the GL equations, so F_i can be calculated by substituting Eq. (47) into Eq. (9) and expanding $g_m \approx 1 - |f_m|^2/2 - |f_m|^4/8$:

$$F_i = \pi q T \sum_{\omega>0} [|f_1 - f_2|^2 + (|f_1|^2 - |f_2|^2)^2/4], \tag{48}$$

where $q = (N_1\gamma_{12} + N_2\gamma_{21})/2$. Combining F_i with F_0 in the dirty limit for $g = 0$ [38], we arrive at the GL free energy $\int F\,\mathrm{d}V$ for $g \ll 1$:

$$\begin{aligned} F = {} & a_1|\Psi_1|^2 + c_{1\alpha}|\Pi_\alpha\Psi_1|^2 + b_1|\Psi_1|^4/2 + a_2|\Psi_2|^2 \\ & + c_{2\alpha}|\Pi_\alpha\Psi_2|^2 + b_2|\Psi_2|^4/2 - a_i\mathrm{Re}(\Psi_1\Psi_2^*) \\ & + c_{i\alpha}\mathrm{Re}(\Pi_\alpha\Psi_1\Pi_\alpha^*\Psi_2^*) - b_i|\Psi_1|^2|\Psi_2|^2 \\ & + 2b_i(|\Psi_1|^2 + |\Psi_2|^2)\mathrm{Re}(\Psi_1\Psi_2). \end{aligned} \tag{49}$$

Here the GL expansion coefficients are given by

$$a_1 = \frac{N_1}{2}\left[\ln\frac{T}{T_1} + \frac{\pi\gamma_{12}}{4T}\right], \tag{50}$$

$$a_2 = \frac{N_2}{2}\left[\ln\frac{T}{T_2} + \frac{\pi\gamma_{21}}{4T}\right], \tag{51}$$

$$c_{1\alpha} = N_1 D_{1\alpha}\left[\frac{\pi}{16T} - \frac{7\zeta(3)\gamma_{12}}{8\pi^2T^2}\right], \tag{52}$$

$$c_{2\alpha} = N_2 D_{2\alpha}\left[\frac{\pi}{16T} - \frac{7\zeta(3)\gamma_{21}}{8\pi^2T^2}\right], \tag{53}$$

$$b_1 = N_1\left[\frac{7\zeta(3)}{16\pi^2T^2} - \frac{3\pi\gamma_{12}}{384T^3}\right], \tag{54}$$

$$b_2 = N_2\left[\frac{7\zeta(3)}{16\pi^2T^2} - \frac{3\pi\gamma_{21}}{384T^3}\right], \tag{55}$$

$$a_i = \frac{N_1}{2}\left[\frac{\lambda_{12}}{w} + \frac{\pi\gamma_{12}}{4T}\right] + \frac{N_2}{2}\left[\frac{\lambda_{21}}{w} + \frac{\pi\gamma_{21}}{4T}\right], \tag{56}$$

$$c_i = \frac{7\zeta(3)}{(4\pi T)^2}(D_1 + D_2)(\gamma_{12}N_1 + \gamma_{21}N_2), \tag{57}$$

$$b_i = \frac{\pi}{384T^3}(\gamma_{12}N_1 + \gamma_{21}N_2), \tag{58}$$

where $T_1 = T_{c0}\exp[-(\lambda_0 - \lambda_-)/2w]$, and $T_2 = T_{c0}\exp[-(\lambda_0 + \lambda_-)/2w]$. The GL equations are obtained by varying $\int F\,\mathrm{d}V$. I would like to point out the misprints with wrong signs of a_i, c_1 and c_2 in Eqs. (13), (14) and (20) in Ref. [38] (see also Ref. [86]).

The first two lines in Eq. (49) are the GL intraband free energies and the term $a_i\mathrm{Re}(\Psi_1\Psi_2^*)$ describes the Josephson coupling of Ψ_1 and Ψ_2. Interband scattering increases a_1 and a_2, and the interband coupling constant a_i. The net result is the reduction of T_c determined by the equation $4a_1(T_c)a_2(T_c) = a_i^2$, which reproduces Eq. (16). Besides the renormalization of a_m, b_m and c_m, interband scattering produces new terms, which describe the mixed gradient coupling and the nonlinear quatric interaction of Ψ_1 and Ψ_2. Similar terms were introduced in the GL theories of heavy fermions [12] and borocarbides [89], and phenomenological models of H_{c2} in MgB_2 [87]. These terms result from interband scattering, so both c_i and b_i vanish in the clean limit [86]. The mixed gradient terms in Eq. (49) produce interference terms in the current density $\mathbf{J} = -c\delta F/\delta\mathbf{A}$:

$$\begin{aligned} \mathbf{J} = {} & -[(2c_1\Delta_1^2 + c_i\Delta_1\Delta_2\cos\theta)\mathbf{Q}_1 + (2c_2\Delta_2^2 + c_i\Delta_1\Delta_2\cos\theta)\mathbf{Q}_2 \\ & + c_i(\Delta_2\nabla\Delta_1 - \Delta_1\nabla\Delta_2)\sin\theta]2\pi c/\phi_0 \end{aligned} \tag{59}$$

where $\mathbf{Q}_m = \nabla\theta_m + 2\pi\mathbf{A}/\phi_0$, and $\theta = \theta_1 - \theta_2$. Here $\mathbf{J}$ is no longer the sum of independent contributions of two bands, because phase gradients in one band produce currents in the other. Moreover, $\mathbf{J}$ acquires new $\cos\theta$ terms and the peculiar $\sin\theta$ interband Josephson-like contribution for inhomogeneous gaps. For currents well below the depairing limit, both bands are phase-locked ($\theta = 0$), and Eq. (59) defines the London penetration depth $\Lambda^2 = c\phi_0 Q/8\pi^2|J|$:

$$\Lambda = \phi_0/4\pi[2\pi(c_1\Delta_1^2 + c_i\Delta_1\Delta_2 + c_2\Delta_2^2)]^{1/2} \tag{60}$$

where c_1, c_2 and c_i depend on the field orientation according to Eq. (44). Eq. (47) can be used to calculate $H_{c2}^{\perp}(T)$ from the linearized GL equations, which give H_{c2} as a solution of the quadratic equation [89]

$$4\left[\frac{2\pi c_1 H}{\phi_0} + a_1\right]\left[\frac{2\pi c_2 H}{\phi_0} + a_2\right] = \left[a_i + \frac{2\pi c_i H}{\phi_0}\right]^2 \tag{61}$$

which reduces to Eq. (27) near T_c to the linear accuracy in $\gamma_{mm'}$. However, the GL calculations of $H_{c2}(T)$ in MgB_2 beyond the linear $T_c - T$ term [87,88] have a rather limited applicability, since $a_1(T)$ and $a_2(T)$ change signs at very different temperatures T_1 and T_2. For λ_{mn} of Ref. [77], $T_1 \sim 0.9T_{c0}$ and $T_2 \sim 0.1T_{c0}$ so higher order gradient terms (automatically taken into account in the Eliashberg/Eilenberger/Usadel based theories) become important. For example, at $T \approx T_1$ where $a_2(T_1) \gg a_1(T)$, retaining the first gradient term $\propto c_2$ requires taking into account a next order term $\sim H^2$ in the first brackets in Eq. (61), which is beyond the GL accuracy. Thus, applying the GL theory in a wider temperature range [87,88] makes it a procedure of unclear accuracy, which can result in a spurious upward curvature in $H_{c2}(T)$ not always present in a more consistent theory (for example, in the dirty limit at $D_1 \simeq D_2$). In addition, the anisotropy of $D_1(\alpha)$ may further limit the applicability of the GL theory for $\mathbf{H}\|ab$, as for $c_1 \gg c_2$ higher order gradient terms in the π band become important [85].

8. Discussion

The remarkable tenfold increase of $H_{c2}(T)$ in C-doped MgB_2 films [25–29] has brought to focus new and largely unexplored physics and materials science of two-gap superconducting alloys. Moreover, the observations of H_{c2} close to the BCS paramagnetic limit poses the important question of how far can H_{c2} be further increased by alloying. This possibility may be naturally built in the band structure of MgB_2, which provides weak interband coupling and weak interband scattering, thus MgB_2 can be alloyed without strong suppression of T_c. For example, for the C-doped MgB_2 film shown in Fig. 1, ρ_n was increased from $\simeq$0.4 μΩ cm to 560 μΩ cm, yet T_c was only reduced down to 35 K [28]. It is the weakness of interband scattering, which apparently makes it possible to take advantage of the very dirty π band to significantly boost H_{c2} in carbon-doped films which typically have $D_\pi \sim 0.1 D_\sigma$. The reasons why scattering in the π band of C-doped MgB_2 films is so much stronger than in the σ band has not been completely understood, but another immediate benefit for high-field magnet applications [37] is that carbon alloying significantly reduces the anisotropy of H_{c2} down to $\Gamma(T) \simeq 1$–2.

Despite many yet unresolved issues concerning the two-gap superconductivity in MgB_2 alloys, H_{c2} of C-doped MgB_2 has already surpassed H_{c2} of Nb_3Sn (see Fig. 1). Given the intrinsic weakness of interband scattering, which enables tuning MgB_2 by selective atomic substitutions on Mg and B sites, there appear to be no fundamental reasons why H_{c2} of MgB_2 alloys cannot be pushed further up toward the strong-coupling paramagnetic limit (1). Thus, understanding the mechanisms of intra and interband impurity scattering in carbon-doped MgB_2, and the competition between scattering and doping effects becomes an important challenge for the computational physics. For instance, it remains unclear why the multiphased C-doped HPCVD grown films [32] exhibit higher H_{c2} and weaker T_c suppression [28] than uniform carbon solid solutions [26,69,70]. This unexpected result may indicate other extrinsic mechanisms of H_{c2} enhancement, which are not included in the simple two-gap theory presented here. Among those may be effects of electron localization or strong lattice distortions in multiphased C-doped films which can manifest themselves in the buckling of the Mg planes observed in the dirty fiber-textured MgB_2 films shown in Fig. 2 [25]. Such buckling may enhance scattering in the π band formed by the out-of-plane p_z boron orbitals.

Recently significant enhancements of vortex pinning and critical current densities J_c in MgB_2 [90–96] have been achieved, particularly by introducing SiC [92] and ZrB_2 [95] nanoparticles. Given these promising results combined with weak current blocking by grain boundaries [97], the lack of electromagnetic granularity [98], and very slow thermally-activated flux creep [99,100], it is not surprising that MgB_2 is being regarded as a strong contender of traditional high-field magnet materials like NbTi and Nb_3Sn. Despite these achievements, a detailed theory of pinning in MgB_2 is still lacking. Such theory should take into account a composite structure of the vortex core, which consists of concentric regions of radius ξ_σ and ξ_π where $\Delta_\sigma(r)$ and $\Delta_\pi(r)$ are suppressed [101–106]. For example, in MgB_2 single crystals the larger vortex cores in the π band start overlapping above the "virtual upper critical field" $H_v = \phi_0/2\pi\xi_\pi^2 \sim 0.5$ T, causing strong overall suppression of Δ_π well below H_{c2} [102,103]. This effect can reduce J_c at $H > H_v$, however both H_v and H_{c2} can be greatly increased by appropriate enhancement of impurity scattering, particularly in the π band, so that $\xi_\pi < \xi_\sigma$.

Recently there has been an emerging interest in microwave response of MgB_2 [107–109] and a possibility of using MgB_2 in resonant cavities for particle accelerators [110,111]. These issues require understanding nonlinear electrodynamics and current pairbreaking in two-gap superconductors [112,113], in particular, band decoupling and the formation of interband phase textures at strong rf currents [16,17].

Acknowledgements

This work was partially supported by in-house research program at NHMFL. NHMFL is operated under NSF Grant DMR-0084173 with support from state of Florida.

References

[1] J. Nagamatsu, N. Nakagawa, T. Muranaka, Y. Zenitani, J. Akimitsu, Nature 410 (2001) 63.
[2] A. Liu, I.I. Mazin, J. Kortus, Phys. Rev. Lett. 87 (2001) 087005.
[3] H.J. Choi, D. Roundy, H. Sun, M.L. Cohen, S.G. Loule, Nature 418 (2002) 758;
H.J. Choi, D. Roundy, H. Sun, M.L. Cohen, S.G. Loule, Phys. Rev. B 66 (2002) R020513.
[4] A. Floris et al., Phys. Rev. Lett. 94 (2005) 037004.
[5] C. Buzea, T. Yamashita, Supercond. Sci. Technol. 14 (2001) R115.
[6] P.C. Canfield, S.L. Bud'ko, D.K. Finnemore, Physica C385 (2003) 1.
[7] H. Suhl, B.T. Matthias, L.R. Walker, Phys. Rev. Lett. 3 (1959) 552.
[8] V.A. Moskalenko, Fiz. Met. Metalloved. 8 (1959) 503 [Sov. Phys. Met. Metallog. 8 (1959) 25];
V.A. Moskalenko, M.E. Palistrat, V.M. Vakalyuk, Usp. Fiz. Nauk 161 (1991) 155 [Sov. Phys. Usp. 34 (1991) 717].
[9] S.V. Shulga, S.-L. Drechsler, G. Fuchs, K.-H. Müller, K. Winzer, M. Heinecke, K. Krug, Phys. Rev. Lett. 80 (1998) 1730;
S.V. Shulga et al. cond-mat/0103154.
[10] V. Guritani, W. Goldacker, F. Bouquet, Y. Wang, R. Lortz, G. Goll, A. Junod, Phys. Rev. B 70 (2004) 184526.
[11] Y. Yokoya, T. Kiss, A. Chainani, S. Shin, M. Mikara, H. Takagi, Science 294 (2001) 2518;
E. Boaknin et al., Phys. Rev. Lett. 90 (2003) 117003.
[12] G. Seyfarth et al., Phys. Rev. Lett. 95 (2005) 107004.
[13] J. Singleton, C. Mielke, Contempor. Phys. 43 (2002) 63.
[14] I.I. Mazin et al., Phys. Rev. Lett. 89 (2002) 107002.
[15] A.J. Legget, Prog. Theor. Phys. 36 (1966) 901;
A.J. Legget, Rev. Mod. Phys. 47 (1975) 331.
[16] A. Gurevich, V.M. Vinokur, Phys. Rev. Lett. 90 (2003) 047004.
[17] A. Gurevich, V.M. Vinokur, Phys. Rev. Lett. 97 (2006) 137003.
[18] T.P. Orlando, E.J. McNiff, S. Foner, M.R. Beasley, Phys. Rev. B 19 (1979) 4545.
[19] A. Godeke, Supercond. Sci. Technol. 19 (2006) R68.

[20] S. Patnaik et al., Supercond. Sci. Technol. 14 (2001) 315.
[21] C.B. Eom et al., Nature 411 (2001) 558.
[22] V. Ferrando et al., Phys. Rev. B 68 (2003) 0945171.
[23] F. Bouquet et al., Physica C 385 (2003) 192.
[24] E. Ohmichi, T. Masui, S. Lee, S. Tajima, T. Osada, J. Phys. Soc. Jpn. 73 (2004) 2065.
[25] A. Gurevich et al., Supercond. Sci. Technol. 17 (2004) 278.
[26] R.T.H. Wilke, S.L. Bud'ko, P.C. Canfield, D.K. Finnemore, R.J. Suplinskas, S.T. Hannahs, Phys. Rev. Lett. 92 (2004) 217003.
[27] A.V. Pogrebnyakov et al., Appl. Phys. Lett. 85 (2004) 2017.
[28] V. Braccini et al., Phys. Rev. B 71 (2005) 012504.
[29] M. Angst, S.L. Budko, R.H.T. Wilke, P.C. Canfield, Phys. Rev. B 71 (2005) 144512.
[30] H.-J. Kim, H.-S. Lee, B. Kang, W.-H. Yim, Y. Jo, M.-H. Jung, S.-I. Lee, Phys. Rev. B 73 (2006) 064520.
[31] P. Samuely, P. Szabo, Z. Holanova, S. Budko, P. Canfield, Physica C435 (2006) 71.
[32] X.X. Xi et al., Supercond. Sci. Technol. 17 (2004) 196.
[33] A.A. Abrikosov, L.P. Gor'kov, Zh. Exper. Teor. Fiz. 36 (1959) 319.
[34] P.G. De Gennes, Phys. Cond. Mater. 3 (1964) 79.
[35] E. Helfand, N.R. Werthamer, Phys. Rev. 147 (1966) 288;
N.R. Werthamer, E. Helfand, P.C. Hohenberg, Phys. Rev. 147 (1966) 295.
[36] K. Maki, Phys. Rev. 148 (1966) 362.
[37] D. Larbalestier, A. Gurevich, D.M. Feldmann, A. Polyanskii, Nature 414 (2001) 368.
[38] A. Gurevich, Phys. Rev. B 67 (2003) 184515.
[39] A.A. Golubov, A.E. Koshelev, Phys. Rev. B 68 (2003) 1045031.
[40] M. Mansor, J.P. Carbotte, Phys. Rev. B 72 (2005) 024538.
[41] This toy model should not be taken too literally, since $H_{c2}(\alpha)$ in real multilayers in an inclined field can depend on the film thickness due to the effect of surfaces on the nucleation of vortices.
[42] L.P. Gor'kov, T.K. Melik-Barkhudarov, JETP 18 (1964) 1031.
[43] L.N. Bulaevskii, Zh. Exp. Teor. Fiz. 64 (1973) 2241;
L.N. Bulaevskii, Zh. Exp. Teor. Fiz. 65 (1973) 1278 [JETP 37 (1973) 1133; 38 (1974) 634].
[44] D.K. Belashchenko, M. van Schilfgaarde, V.P. Antropov, Phys. Rev. B 64 (2001) 092503.
[45] I.I. Mazin, V.P. Antropov, Physica C 385 (2003) 49.
[46] S.L. Bud'ko, V.G. Kogan, P.C. Canfield, Phys. Rev. B 64 (2001) 180506.
[47] S. Lee, H. Mori, T. Masui, Y. Eltsev, A. Yamamoto, S. Tajima, J. Phys. Soc. Jpn. 70 (2001) 2255.
[48] S.L. Bud'ko, P.C. Canfield, Phys. Rev. B 65 (2002) 212501.
[49] A.K. Pradhan et al., Phys. Rev. B 64 (2001) 212509.
[50] M. Angst et al., Phys. Rev. B 88 (2002) 167004.
[51] A.V. Sologubenko, J. Jun, S.M. Kazakov, J. Karpinski, H.R. Ott, Phys. Rev. B 65 (2002) 180505.
[52] K. Takahashi, T. Atsumi, N. Yamamoto, M. Xu, H. Kitazawa, T. Ishida, Phys. Rev. B 66 (2002) 012501.
[53] M. Zehetmayer, M. Eisterer, J. Jun, S.M. Kazakov, J. Karpinski, A. Wisniewski, H.W. Weber, Phys. Rev. B 66 (2002) 052505.
[54] S.L. Bud'ko, P.C. Canfield, V.G. Kogan, Physica C 387 (2002) 85.
[55] A. Rydh et al., Phys. Rev. B 70 (2004) 132503.
[56] L. Lyard et al., Phys. Rev. Lett. 92 (2004) 057001.
[57] V.G. Kogan, Phys. Rev. B 66 (2002) 020509.
[58] T. Dahm, N. Schopohl, Phys. Rev. Lett. 91 (2003) 017001.
[59] J. Kortus, O.V. Dolgov, R.K. Kremer, A.A. Golubov, Phys. Rev. Lett. 94 (2005) 027002.
[60] M. Putti et al., Phys. Rev. B 70 (2004) 052509;
M. Putti et al., Phys Rev. B 71 (2005) 144505.
[61] R.J. Cava, H.W. Zandbergen, K. Inumaru, Physica C 385 (2003) 8.
[62] R.A. Ribeiro, S.L. Bud'ko, C. Petrovic, P.C. Canfield, Physica C 385 (2003) 16.
[63] J. Karpinski et al., Supercond. Sci. Technol. 16 (2003) 221.
[64] J. Kim, R.K. Singh, N. Newman, J.M. Rowell, IEEE Trans. Appl. Supercond. 13 (2003) 3238.
[65] G.K. Perkins et al., Nature 411 (2001) 561.
[66] M. Eisterer et al., Supercond. Sci. Technol. 15 (2002) L9.
[67] Y. Wang et al., J. Phys.: Condens. Matter 15 (2003) 883.
[68] R. Gandikota et al., Appl. Phys. Lett. 86 (2005) 012508.
[69] S. Lee, T. Masui, A. Yamamoto, H. Uchiyama, S. Tajima, Physica C 397 (2003) 7.
[70] T. Masui, S. Lee, S. Tajima, Phys. Rev. B 70 (2004) 0245041.
[71] T. Kakeshita, S. Lee, S. Tajima, Phys. Rev. Lett. 97 (2006) 037002.
[72] G. Sarma, J. Phys. Chem. Solids 24 (1963) 1029.
[73] M. Schossmann, J.P. Carbotte, Phys. Rev. B 39 (1989) 4210.
[74] H.J. Nui, D.P. Hampshire, Phys. Rev. Lett. 91 (2003) 027002.
[75] R.A. Klemm, A. Luther, M.R. Beasley, Phys. Rev. B 12 (1975) 877.
[76] S. Takachashi, M. Tachiki, Phys. Rev. B 33 (1968) 4620.
[77] A.A. Golubov et al., J. Phys: Condens. Matter 14 (2002) 1353.
[78] F_i of Ref. [17] should be multiplied by $-1/2$.
[79] N. Schophol, K. Scharnberg, Solid State Commun. 22 (1977) 371.
[80] A.A. Golubov, I.I. Mazin, Phys. Rev. B 55 (1997) 15146.
[81] M. Iavarone et al., Phys. Rev. B 71 (2005) 214502.
[82] M. Tinkham, Phys. Rev. B 129 (1963) 2413.
[83] V.G. Kogan, Phys. Rev. B 66 (2002) R020509;
V.G. Kogan, N. Zhelezina, Phys. Rev. B 69 (2004) 1235061.
[84] A.A. Golubov, A. Brinkman, O.V. Dolgov, J. Kortus, O. Jepsen, Phys. Rev. B 66 (2002) 054524.
[85] A.A. Golubov, A.E. Koshelev, Phys. Rev. Lett. 68 (2003) 104503.
[86] M.E. Zhitomirsky, V.H. Dao, Phys. Rev. B 69 (2004) 054508.
[87] I.N. Askerzade, A. Gencer, N. Güclú, Supercond. Sci. Technol. 15 (2002) L13;
I.N. Askerzade, Physica C 390 (2003) 281.
[88] V.H. Dao, M.E. Zhitomirsky, Eur. J. Phys. 44 (2005) 183.
[89] H. Doh, M. Sigrist, B.K. Cho, S.-I. Lee, Phys. Rev. Lett. 83 (1999) 5350.
[90] A. Gümbel, J. Eckert, G. Fuchs, K. Nenkov, K.H. Müller, L. Schultz, Appl. Phys. Lett. 80 (2002) 2725.
[91] K. Komori et al., Appl. Phys. Lett. 81 (2002) 1047.
[92] S.X. Dou et al., Appl. Phys. Lett. 81 (2002) 3419.
[93] J. Wang et al., Appl. Phys. Lett. 81 (2002) 2026.
[94] R. Flukiger, H.L. Suo, N. Musolino, C. Beneduce, P. Toulemonde, P. Lezza, Physica C 385 (2003) 286.
[95] M. Bhatia, M.D. Sumption, E.W. Collings, S. Dregia, Appl. Phys. Lett. 87 (2005) 042505.
[96] B.J. Senkowicz, J.E. Giencke, S. Patnaik, S.B. Eom, E.E. Hellstrom, D.C. Larbalestier, Appl. Phys. Lett. 86 (2005) 202502.
[97] D.C. Larbalestier et al., Nature 410 (2001) 186.
[98] A.A. Polyanskii et al., Supercond. Sci. Technol. 14 (2001) 811.
[99] J.R. Thompson, M. Paranthaman, D.K. Christen, K.G. Sorge, J.G. Ossandon, Supercond. Sci. Technol. 14 (2001) L17.
[100] S. Patnaik, A. Gurevich, S.D. Bu, J. Choi, C.B. Eom, D.C. Larbalestier, Phys. Rev. B 70 (2004) 064503.
[101] E. Babaev, Phys. Rev. Lett. 89 (2002) 0670011.
[102] M.R. Eskildsen et al., Phys. Rev. Lett. 89 (2002) 187004-4.
[103] S. Serventi et al., Phys. Rev. Lett. 93 (2004) 217003.
[104] A.E. Koshelev, A.A. Golubov, Phys. Rev. Lett. 90 (2003) 177002.
[105] M. Ichioka, K. Machida, N. Nakai, P. Miranovic, Phys. Rev. B 70 (2004) 1445081.
[106] A. Guman, S. Graser, T. Dahm, N. Schopohl, Phys. Rev. B 73 (2006) 104506.
[107] A.T. Findikoglu et al., Appl. Phys. Lett. 83 (2003) 108.
[108] B.B. Jin et al., Appl. Phys. Lett. 87 (2005) 092503.
[109] G. Cifaiello et al., Appl. Phys. Lett. 88 (2006) 142510.
[110] E.W. Collings, M.D. Sumption, T. Tajima, Supercond. Sci. Technol. 17 (2004) 595.
[111] A. Gurevich, Appl. Phys. Lett. 88 (2006) 12511.
[112] M.N. Kunchur, J. Phys. Condens. Matter 16 (2004) R1183.
[113] E.J. Nicol, J.P. Carbotte, D.J. Scalapino, Phys. Rev. B 73 (2006) 014521.